DOE/ET-53088-58 IFSR #58R

DRIFT WAVE TURBULENCE IN A LOW ORDER $\underset{\sim}{k}$ SPACE

P. W. Terry
and
W. Horton

Institute for Fusion Studies

March 1982

(Revised December 1982)

Drift Wave Turbulence in a Low-Order $\underset{\sim}{k}$ Space

P.W. Terry and W. Horton

Institute for Fusion Studies

University of Texas at Austin

Austin, Texas 78712

Abstract

In the low order isotropic $\underset{\sim}{k}$ space introduced by Kells and Orszag for the two dimensional Euler equation, we study the evolution of the fluctuations arising from the electron drift wave instability. The two dimensional drift wave model contains the $\underset{\sim}{E} \times \underset{\sim}{B}$ and polarization drift nonlinearities in the hydrodynamic ions and linear, dissipative electrons. The strength of the electron dissipation is shown to determine the spectral width and the level of the fluctuations.

March 1982

(Revised December 1982)

To be published in the Physics of Fluids

I. Introduction

Low order systems as models for turbulence have received considerable attention in recent years.[1-9] A low order system of particular interest in plasma physics has been a model for the interaction of an unstable mode with two damped modes.[5-9] For the decay of an unstable mode into a damped subharmonic the system is three-dimensional, and extensive studies[5-7] have established the existence of turbulent-like regimes of behavior due to the presence of a strange attractor. In studying the three-wave interaction for drift waves two important generalizations are necessary. First the triplet interactions require a four dimensional system since the decay into a subharmonic is forbidden, and secondly the mode coupling coefficients are intrinsically complex when dissipation is introduced self-consistently into the dynamical equation.[8,9,10] The dissipative drift wave triplet shows chaotic behavior in typical interaction triangles, with comparable growth and damping rates, in contrast to the subharmonic decay problem which requires a large ratio ($\sim$20) of damping-to-growth for the onset of stochasticity. The stochastic regime of the four dimensional drift wave triplet is characterized by random phases and amplitudes for waves with comparable frequencies and growth rates. Typically, the frequency spectra of all three modes are broad; the amplitudes of the electrostatic fluctuations in the saturated state are unrealistically high ($\tilde{\phi} \sim 50$ being typical for a randomly chosen drift wave triplet).

Inasmuch as the three drift wave interaction problem is a paradigm for drift wave turbulence, it becomes desirable to test its conclusions for cases with a larger number of modes. To this end, we investigate here the nature of drift wave turbulence as modeled by the interaction of the lowest number of modes greater than three such that the modes comprise an

isotropically distributed set in $\underset{\sim}{k}$ space. In this approach we follow the work of Kells and Orszag[4] who investigate the lowest order isotropically truncated two dimensional $\underset{\sim}{k}$ spaces for the Euler equation describing inviscid, incompressible flow in neutral fluids. They introduce four truncated $\underset{\sim}{k}$ space models of which the general lowest order model, requires the evolution of twenty modes (twenty-first order differential equations).

In our study of the drift wave instability in the low order $\underset{\sim}{k}$ space we consider the frequency and wavenumber spectrum of the turbulence. Having found in the triplet interaction a condition on the linear growth and damping such that saturation of the instability occurs, we seek such a condition in the interaction of twenty modes.

We show that the system parameters can be varied to range from frequency spectra peaked near the linear frequencies to very broad frequency spectra. We wish to consider the variation of the spectral width as a function of the mean amplitude of the saturated turbulence to compare with the predictions of weak turbulence theory, renormalized turbulence theory and with the electromagnetic scattering experiments. We show that the strength of the dissipation in the system is instrumental in determining the frequency width versus amplitude dependence. Finally, we make a few observations regarding the anisotropy of the $\underset{\sim}{k}$ spectrum.

II. The Drift Wave Model and the Truncated $\underset{\sim}{k}$ Space

We use a two fluid description of the electron drift waves containing the $\underset{\sim}{E} \times \underset{\sim}{B}$ convective nonlinearity in the hydrodynamic ions and using linear, dissipative electrons. The dynamical equation for the evolution of the electrostatic potential $\phi(\underset{\sim}{x},t)$ is obtained from the statement of

quasineutrality. In the limit of low ion pressure the ion density evolution is governed by the continuity equation

$$\frac{\partial n_i}{\partial t} + \underset{\sim}{v}_E \cdot \nabla n_i + \nabla \cdot (n_i \underset{\sim}{v}_p) = 0 \tag{1}$$

with the incompressible $\underset{\sim}{E} \times \underset{\sim}{B}$ convective velocity

$$\underset{\sim}{v}_E = \left(\frac{cT_e}{eB}\right) \hat{b} \times \nabla\phi \tag{2}$$

and the compressible, nonlinear polarization drift

$$\underset{\sim}{v}_p = \underset{\sim}{v}_p^{\ell} + \underset{\sim}{v}_p^{n\ell} = -\rho^2\left(\frac{\partial}{\partial t} + \underset{\sim}{v}_E \cdot \nabla\right)\nabla_\perp\phi \tag{3}$$

where the electrostatic potential ϕ is measured in units of the electron temperature T_e/e and the ion inertial scale length is given by $\rho = c(m_i T_e)^{1/2}/eB$.

The electron dynamics is linear and taken from the $\underset{\sim}{k}$ space dependence of the linear Vlasov response to the drift wave. For a fixed parallel wavenumber determined by the geometry, such as $|k_\parallel| = 1/qR$ for a tokamak, the two dimensional electron density response is given approximately by

$$n_e(\underset{\sim}{x},t) = n_e(x)[1 + \phi(\underset{\sim}{x},t) + \mathcal{L}^a\phi(\underset{\sim}{x},t)] \tag{4}$$

where the anti-hermitian operator $\mathcal{L}^a$ gives the dissipation responsible for the drift wave instabilitiy. For the collisionless electron-wave resonance we have

$$\mathcal{L}^a(\underset{\sim}{k}) = i\,\delta_0 k_y\left(k_\perp^2 - \frac{1}{2}\eta_e\right) \tag{5}$$

from the Fourier transform of $\mathcal{L}^a$ where

$$\delta_0 = \left(\frac{\pi}{2}\right)^{1/2}\left(\frac{m_e}{m_i}\right)^{1/2}\left[\frac{1}{|k_\parallel| r_n}\right] .$$

The constant δ_0 determines the strength of dissipation in the model and is of order unity for strong instability.

In writing Eq. (5) we define $r_n^{-1} = -d_x \ell n\, n_e(x)$ and $\eta_e = d_x \ell n\, T_e(x)/d_x \ell n\, n_e(x)$ and introduce the dimensionless space-time variables in units of ρ and r_n/c_s where $c_s = (T_e/m_i)^{1/2}$ is the ion-acoustic speed. We now rescale the dimensionless potential by $\phi \Longrightarrow (\rho/r_n)\phi$ to obtain unit strength for the nonlinear coupling. For example, $\nabla \cdot \underset{\sim}{v}_p = -\nabla_\perp^2\, \partial_t \phi(\underset{\sim}{x},t) - \hat{b} \times \nabla\phi \cdot \nabla\nabla_\perp^2\phi$ in these dimensionless variables. The form of the operator $\mathcal{L}^a(\underset{\sim}{k})$ in other regimes is given in Ref. 8, Appendix A where a more detailed derivation of the mode coupling equations may also be found.

We eliminate the plasma density through quasineutrality to obtain the nonlinear partial differential equation[10,11] governing the electrostatic potential

$$(1 + \mathcal{L})\,\frac{\partial \phi(x,y,t)}{\partial t} = -\frac{\partial \phi}{\partial y} - [\phi, \mathcal{L}\phi] \tag{6}$$

where $\mathcal{L} = -\nabla_\perp^2 + \mathcal{L}^a$ and

$$[g,h] = \hat{b} \cdot \nabla g \times \nabla h = \frac{\partial g}{\partial x}\frac{\partial h}{\partial y} - \frac{\partial h}{\partial x}\frac{\partial g}{\partial y} \quad ,$$

$$\mathcal{L}^a = \delta_0(\nabla_\perp^2 + \frac{1}{2}\eta_e)\frac{\partial}{\partial y} \, .$$

We write the convective nonlinearity in terms of the Poisson brackets [g,h] to emphasize the conservation properties of the mode coupling: $\int [g,h]d\underset{\sim}{x} = \int g[g,h]d\underset{\sim}{x} = \int h[g,h]d\underset{\sim}{x} = 0$. The two dimensional nonlinear partial differential Eq. (6) for $\phi(\underset{\sim}{x},t)$ and Eq. (4) for $n_e(\underset{\sim}{x},t)$ describe the evolution of the plasma fluctuations in the presence of frozen density and temperature gradients. The mean value $\langle\phi\rangle$ of the fluctuations remains zero throughout time. The fluctuations are described by the root-mean-square level $\tilde{\phi} = \langle\phi^2\rangle^{1/2}$ and their spectral components $|\phi_{\underset{\sim}{k}}(\omega)|$.

We introduce the Galerkin approximation of $\phi(x,y,t)$ through the truncated Fourier series

$$\phi(\underset{\sim}{x},t) = \sum_{|\underset{\sim}{k}|\leq K} \phi_{\underset{\sim}{k}}(t)\exp(i\underset{\sim}{k}\cdot\underset{\sim}{x}) \qquad (7)$$

where $\underset{\sim}{k} = (k_x,k_y)$. We take k_x and k_y to be integral multiples of k_0 and define K as the wavenumber cutoff. Transforming Eq. (6) to a set of equations for $\phi_{\underset{\sim}{k}}(t)$ we obtain

$$(1+\chi_{\underset{\sim}{k}})\frac{d\phi_{\underset{\sim}{k}}}{dt} = -ik_y\phi_{\underset{\sim}{k}} + \frac{1}{2}\sum_{\substack{\underset{\sim}{k}_1+\underset{\sim}{k}_2=\underset{\sim}{k} \\ |\underset{\sim}{k}_1|,|\underset{\sim}{k}_2|\leq K}} (\underset{\sim}{k}_1 \times \underset{\sim}{k}_2 \cdot \hat{b})(\chi_{\underset{\sim}{k}_2} - \chi_{\underset{\sim}{k}_1})\phi_{\underset{\sim}{k}_1}\phi_{\underset{\sim}{k}_2} \qquad (8)$$

where $(\mathcal{L}\phi)_{\underset{\sim}{k}} = \chi_{\underset{\sim}{k}}\phi_{\underset{\sim}{k}}$ is the complex susceptibility given by

$$\chi_{\underset{\sim}{k}} = k_\perp^2 - i\delta_0 k_y(k_\perp^2 - \frac{1}{2}\eta_e) \qquad (9)$$

which determines the linear frequency dispersion and the dissipation.

In the dissipationless limit and with no adiabataic electron shielding, the function $\chi_{\underset{\sim}{k}}$ becomes $1 + \chi_{\underset{\sim}{k}} \to \underset{\sim}{k}^2$, and the mode coupling Eq. (8) reduces to the two dimensional Euler equation in the form studied by Kells and Orszag.[4] In that work four $\underset{\sim}{k}$ space truncation models (A,B,C,D) are investigated as alternative low order representation of the partial differential equation. In the present work we adopt their model C where $K = (5)^{1/2}k_0$.

This truncation model yields twenty modes ($\underset{\sim}{k} = 0$ excluded) and constitutes the smallest nondegenerate isotropically distributed $\underset{\sim}{k}$ space truncation according to Kells and Orszag. Smaller values of K/k_0 yield a collection of modes whose interactions break up into that of isolated triplets. The condition of reality of the electrostatic potential $\phi(x,y,t)$ requires $\phi_{\underset{\sim}{k}}(t) = \phi^*_{\underset{\sim}{k}}(t)$ so that ten complex modes in the one half plane need to be advanced in time. Figure 1 shows the truncated $\underset{\sim}{k}$ space with the labels we assign to each mode. The system is advanced in time by integrating twenty real equations for $y_{2\ell-1} = \mathrm{Re}[\phi_\ell(t)]$ and $y_{2\ell} = \mathrm{Im}[\phi_\ell(t)]$.

A related system of drift wave mode coupling equations has been considered recently by Waltz.[12] His studies include a variable number of $\underset{\sim}{k}$ space modes and alternative forms of the linear growth and damping formulas.

III. Properties of the Truncated System

Several important physical properties of the system of equations (8) and (9) are now discussed.

A. Linear Modes

The model describes the linear electron drift wave instability with the frequency dispersion given by

$$\omega(\underset{\sim}{k}) \cong \frac{k_y}{1 + k_\perp^2} \tag{10a}$$

and the growth and damping of the linear waves given by

$$\gamma(k) \cong \frac{\delta_0 k_y^2 (k_\perp^2 - \frac{1}{2}\eta_e)}{(1 + k_\perp^2)^2} \quad . \tag{10b}$$

[The exact complex linear frequency is $k_y/(1 + k_\perp^2 + \mathcal{L}^a(\underset{\sim}{k}))]$. For $k_0^2 < \frac{1}{2}\eta_e < K^2$ there are both growing and damped modes to model the physical systems of interest.

The energy density of the drift wave is due to the electrostatic energy $-e\delta n_e \phi$ in the adiabatic electrons and the kinetic energy $\frac{1}{2} n m_i v_E^2$ in the ion drifts. In these units the energy for each mode is $W(\underset{\sim}{k}) = \frac{1}{2}(1+k_\perp^2)|\phi(\underset{\sim}{k})|^2$, and the total energy is

$$W(t) \equiv \frac{1}{2} \sum_{|\underset{\sim}{k}| \leq K} (1+k^2) |\phi_{\underset{\sim}{k}}(t)|^2. \tag{11}$$

The measure of the average vorticity $\nabla \times \underset{\sim}{v}$ in the flow is given by the enstrophy. We define the potential enstrophy U by

$$U(t) = \frac{1}{2} \sum_{|\underset{\sim}{k}| \leq K} k^2(1+k^2) |\phi_{\underset{\sim}{k}}(t)|^2 \quad . \tag{12}$$

For reference we note that the total physical energy density in the waves is given by $(\rho/r_n)^2 n_e T_e \, W(t)$.

B. Conservation Properties of $\underset{\sim}{E} \times \underset{\sim}{B}$ Coupling

The nonlinearity of the system arises from the $\underset{\sim}{E} \times \underset{\sim}{B}$ convection of the plasma density and the ion velocity field $\underset{\sim}{v}_E$. The convection mixes the plasma and in the process transfers energy between modes $\underset{\sim}{k}_1 + \underset{\sim}{k}_2 = \underset{\sim}{k}$ without dissipation. In Eq. (8) the conservation properties follow from $\sum_{\underset{\sim}{k}} \sum_{\underset{\sim}{k}_1+\underset{\sim}{k}_2=\underset{\sim}{k}} (\chi_{\underset{\sim}{k}_2} - \chi_{\underset{\sim}{k}_1}) = 0$ and $\sum_{\underset{\sim}{k}} \sum_{\underset{\sim}{k}_1+\underset{\sim}{k}_2} \chi_{\underset{\sim}{k}}(\chi_{k_2} - \chi_{\underset{\sim}{k}_1}) = 0$, which are satisfied for each triplet $\underset{\sim}{k}_1 + \underset{\sim}{k}_2 = \underset{\sim}{k}$ in the interaction.

In the absence of dissipation $|\mathcal{L}^a| \simeq \delta_0 \equiv 0$ both the energy W and the potential enstrophy are exact constants of the motion. If we arbitrarily set $\gamma_{\underset{\sim}{k}} = 0$ but retain Im $\chi_{\underset{\sim}{k}} \neq 0$ the energy W is constant while the enstrophy undergoes fluctuations.

In the general case of interest to drift wave turbulence both the energy and the enstrophy fluctuate in time. Figure 2 shows a typical evolution of the energy and enstrophy for the linearly unstable system ($n_e = 1$ and $k_0 = 0.33$). The initial state is randomly phased with $|\phi_{\underset{\sim}{k}}| = 0.1$.

C. Phase Space Contraction

In the rectangular Cartesian phase space composed of the real $y_{2\ell-1} = \mathrm{Re}[\phi_{\underset{\sim}{k}}(t)]$ and imaginary $y_{2\ell} = \mathrm{Im}[\phi_{\underset{\sim}{k}}(t)]$ parts of the field variables $\phi_{\underset{\sim}{k}}(t)$, the rate of change of a volume V of systems is given by the divergence of the velocity vector dy_i/dt. For the present system of equations the rate of change of phase space volume is given by

$$\frac{1}{V}\frac{dV}{dt} = \sum_{i=1}^{20} \frac{\partial}{\partial y_i}\left(\frac{dy_i}{dt}\right) = 2\sum_{\ell=1}^{10} \gamma_\ell \equiv 2\gamma_t \quad . \tag{13}$$

The phase space flow is volume contracting when the total dissipation γ_t is negative.

The question of the time-asymptotic boundedness of the solutions may be addressed by considering the stability, or perhaps more precisely the local Lyapunov characteristic exponents, about an arbitrary point in phase space. Local stability to a perturbation $\delta y_i \exp(\lambda t)$ is determined from the roots of the twentieth order secular equation of the eigenvalue problem for the matrix $\left(M_{ij}\right)$ of linearized equations. The problem of obtaining necessary and sufficient conditions from the coefficients of the secular equation $\sum_{n=0}^{20} a_n \lambda^n = 0$ is conceptually straightforward; however, impractical for actual evaluation. We observe, however, that the coefficients M_{jk} of the linearized equations $\delta\dot{y}_j = M_{jk}\delta y_k$ are real so that the eigenvalues λ are either real or complex conjugate pairs. We also may show that due to $\sum_{\underset{\sim}{k}} [\omega(\underset{\sim}{k}) + i\gamma(\underset{\sim}{k})] = 2\gamma_t$, that the trace of matrix is

$$\mathrm{Tr}(M) = 2\gamma_t \quad . \tag{14}$$

Since the secular equation $\sum_{0}^{20} a_n\lambda^n = 0$ has $a_{20} = 1$ and $a_{19} = -\mathrm{Tr}(M) = -2\gamma_t$

independent of the position in phase space, it follows that a necessary condition for stability is that the system be volume contracting.

Numerical simulations for various values of γ_t indicate that the condition $\gamma_t < 0$ is close to being a sufficient condition for stability as well. The evidence for this important conclusion is summarized in Fig. 3 which shows the mean saturation amplitude for the largest amplitude mode in the system as a function of γ_t. We note that there is a critical value γ_t^*, with $\gamma_t^* \sim -0.1$, below which ($\gamma_t < \gamma_t^*$) the amplitudes are found to saturate at successively lower levels as γ_t decreases (taking on larger negative values) and above which no saturation is observed. For $\gamma_t > \gamma_t^*$ we observe exponential growth of W(t). Thus, we conclude from a practical point of view that $\gamma_t < \gamma_t^* \lesssim 0$ is a necessary and sufficient condition for saturation.

D. Symmetries in $\underset{\sim}{k}$ Space

The mode coupling equation possesses a symmetry in $k_x \to -k_x$. Considering Eqs. (8) and (9) for $k_x \to -k_x$ we see that for each solution $\phi(k_x,k_y)$ there is a solution with the properties

$$\phi(-k_x,k_y) = -\phi(k_x,k_y) \tag{15}$$

and

$$\phi(k_x,-k_y) = -\phi^*(k_x,k_y) \tag{16}$$

where property (16) follows from property (15) and the reality condition $\phi_{-\underset{\sim}{k}} = \phi^*_{\underset{\sim}{k}}$. Initial data satisfying conditions (15) and (16) at $t = t_0$ remain symmetric for all $t > t_0$. This property was used as a check on the

simulation code, as well as the constancy of W and U in the $\delta_0 = 0$ limit. Physically, the symmetry guarantees solutions of the form $\sin(k_x x)\cos(k_y y - \omega_{\underset{\sim}{k}} t)$, i.e. separable solutions in x and y representing standing waves in the x direction. A restricted set of mode simulations with standing waves as the basis function in the Garlekin expansion is used in the hydrodynamic studies where boundary conditions $v_x(0,y,t) = v_x(L,y,t) = 0$ are invoked. In contrast we consider systems that are doubly periodic in x and y (without symmetry).

IV. Simulations

A variety of numerical simulations are performed to obtain information on the character of the frequency spectrum, the wavenumber spectrum and the saturation amplitudes. Figure 2 shows the time history of the energy W(t) and the enstrophy U(t) for a typical simulation with $\eta_e = 1.0$ and $\delta_0 = 5.0$. The energy fluctuates about the mean value $\bar{W} = 74$ with $\Delta W \simeq 30$. The root-mean-square potential fluctuation in the saturated state is $\langle\phi^2\rangle^{1/2} = 2.7$ in units of $(\rho/r_n)(T_e/e)$.

The simulations show that both the qualitative and quantitative behavior of the system is sensitive to the amount of dissipation and energy absorption in the system. The ratio of instability due to free energy in the plasma density gradient to the wave absorption may be varied in the simulations by the parameter η_e. We note from Eq. (10b) for $\gamma(\underset{\sim}{k})$ that decreasing η_e increases the growth rate of the unstable modes, and decreases the damping of stable modes. A convenient measure of the ratio of wave emission to wave absorption is γ_t, the total growth rate. A dependence of the system on this ratio is evident in Fig. 3 where increasing the absorption as measured by γ_t makes the amplitude of the dominant mode

decrease from 16 to a few tenths as γ_t varies from -0.12 to -0.45. On this basis we identify weakly and strongly unstable systems. Qualitatively, the system varies with γ_t from a state where the amplitudes fail to saturate, growing exponentially, for small γ_t to a state of small amplitude coherent oscillations about a fixed point attractor for $\gamma_t \leq -0.4$.

Figure 4 shows the time signals of (a) the fastest growing linear mode $\phi_7(t)$ which is the principal source of wave energy and (b) the dominant mode $\phi_9(t)$ in the fluctuating steady state for a weakly unstable case. In Fig. 4a we see the exponential growth of the signal at the rate of γ_7 followed by a chaotic saturated amplitude with a root-mean-square amplitude of $\tilde{\phi}_7 = 4.53$. In Fig. 4b the signal remains small until driven up by the coupling to ϕ_7 at $t \simeq 130$, whereupon it quickly reaches a steady state with $\tilde{\phi}_9 = 5.37$. The evolution of the potential shown here is qualitatively similar to that of the three mode interactions.[8] We note, however, that the mean amplitudes at saturation are considerably lower in the twenty mode system than for a typical three mode interaction.

A unique stationary wavenumber spectrum is established in this system in the saturated state. The time averaged spectrum $W(\underset{\sim}{k})$ is shown in Fig. 5 for a given set of initial data. We find that this same spectrum is obtained for different initial data where we choose $\phi_{\underset{\sim}{k}}(0) = 10^n \exp(i\alpha_{\underset{\sim}{k}})$ with $\alpha_{\underset{\sim}{k}}$ randomly distributed and $-2 \leq n \leq 2$. The stability of the time averaged state is also tested by making large variations $y \to y + \Delta y$ at arbitrary times in the evolution. The randomly phased initial state <u>does not</u> have the symmetries (15) and (16) but evolves into the saturated energy spectrum which is approximately symmetric in $k_x \to -k_x$. The symmetry is due to the dependence of the growth rate and susceptibility on k_x^2.

Figure 5 shows that the energy spectrum is approximately of the form $W(k_x^2, k_y)$ and peaks at the large k_x mode ϕ_9 (with $\gamma_9 = +0.01$) rather than the fastest linearly growing mode ϕ_7 (with $\gamma_7 = +0.04$). A similar behavior is observed in a different drift wave simulation.[13] The rotation of the peak of the energy spectrum from the fastest growing linear mode to the large k_x mode is produced by the $\underset{\sim}{k}_1 \times \underset{\sim}{k}_2 \cdot \hat{b}$ convection coupling which is strongest for the angle of $\pi/2$ between $\underset{\sim}{k}_1$ and $\underset{\sim}{k}_2$.

To investigate further the isotropizing effect of the $\underset{\sim}{k}_1 \times \underset{\sim}{k}_2 \cdot \hat{b}$ coupling process we restart the simulation using the final anisotropic spectrum of Fig. 5 as new initial data. In the restart we eliminate the anisotropic driving force by setting $\gamma_{\underset{\sim}{k}} = 0$ for all modes. The initially anisotropic spectrum relaxes to an approximately isotropic spectrum with the same energy $W = 40$ after $\Delta t = 2000$, as shown in Fig. 6.

Figures 7 and 8 show the frequency spectra of both the fastest growing linear mode ϕ_7 and the dominant mode ϕ_9 for weakly unstable and strongly unstable cases, respectively. In the weakly unstable case, the spectra have sharply defined peaks which lie slightly above the linear frequency. The linear frequencies of ϕ_7 and ϕ_9 are respectively $\omega \approx .43$ and $.22$ while the spectra peak at $.50$ and $.28$. In the strongly unstable case the spectra also appear to peak in the vicinity of the linear frequency; however, the peaks are broadly defined.

The frequency spectra are quantitatively described by a nonlinear regression analysis minimizing the variance about an assumed parametrization of the spectrum with a peak at $\omega_{\underset{\sim}{k}}^{n\ell}$, a width $\nu_{\underset{\sim}{k}}$, and area $\tilde{\phi}_{\underset{\sim}{k}}$ or $I(\underset{\sim}{k})$. Parametrizations with Lorentzian and Gaussian fits to $\phi_{\underset{\sim}{k}}(\omega)$ and $|\phi_{\underset{\sim}{k}}(\omega)|^2$ have been studied. No clear picture of a best parametrization has emerged from the comparisons. Plasma turbulence theory is often formulated in terms

of $|\varepsilon^{nl}(\underset{\sim}{k},\omega)|^2 I_{\underset{\sim}{k}}(\omega) = S_{\underset{\sim}{k}}(\omega)$ with the expansion of the nonlinear dielectric function $\varepsilon^{nl}_{\underset{\sim}{k}}(\omega)$ about $\omega^{nl}(\underset{\sim}{k})$ Neglecting the ω dependence of the source $S_{\underset{\sim}{k}}(\omega)$ yields an Lorentzian approximation to $|\phi_{\underset{\sim}{k}}(\omega)|^2$. Both parametrizations are adequate for fiting the central peaked region. From the fit in the wings however, a decided preference is evident. For nonzero dissipation (δ_0 in excess of a few tenths) the Lorentzian is a better fit. In the absence of dissipation in the mode coupling ($\delta_0 = 0$) the Gaussian approximation is preferred. Both fits however, give the same numerical value for the linewidth ν_k and the peak value ω^{nl}_k to within a standard deviation. Figure 9 summarizes the dependence of the linewidth on the degree of instability by plotting the linewidth ν_k as a function of the saturation amplitude for the dominant mode. We note that turbulence theory predicts that $\nu_k \propto \langle\phi^2\rangle$ for small $\langle\phi^2\rangle$ and $\nu_k \propto \langle\phi^2\rangle^{1/2}$ for large $\langle\phi^2\rangle$. The predictions are borne out by the data shown in Fig. 9. Note that the transition point is given approximately by $\nu_k \simeq \omega_k$ consistent with turbulence theory. The coefficients of proportionality for the two regimes are given by the dashed curves in Fig. 9.

The spectra linewidth $\nu_{\underset{\sim}{k}}$ depends on the dissipation. We recall that the dissipation introduced by the anti-hermitian operator in Eq. (5) scales with the parameter δ_0. For $\delta_0 = 0$ there is no dissipation, the energy and enstrophy are conserved, and the system becomes the drift wave analog of Kells and Orszag's model C. In this limit we also observe equipartition of the wave energy density $W(\underset{\sim}{k}) = W_0 =$ constant, a state analyzed in detail with the microcanonical and canonical ensemble by Kells and Orszag. At small to moderate values of δ_0 the frequency spectra are well approximated by the Lorentzian.

The observed frequency width $\nu_{\underset{\sim}{k}}$ of the mode $\phi_{\underset{\sim}{k}}(t)$ can be interpreted physically in terms of the random Doppler shifts produced by the turbulent flow $\underset{\sim}{v}_E(\underset{\sim}{x},t)$. Recalling that the linear mode frequency $\omega_{\underset{\sim}{k}}$ applies in the rest frame of the ions, the laboratory frame frequency is $\omega_{\underset{\sim}{k}} + \underset{\sim}{k} \cdot \underset{\sim}{v}_E$ due to ion velocity $\underset{\sim}{v}_E$. For slowly varying $\underset{\sim}{v}_E(\underset{\sim}{x},t)$ the laboratory frequency has a low frequency modulation. For high frequency stochastic $\underset{\sim}{v}_E$ there is dispersion of the laboratory frequency given by $\langle(\underset{\sim}{k} \cdot \underset{\sim}{v}_E)^2\rangle$ leading to the turbulent Doppler shift formula

$$\nu_D(\underset{\sim}{k}) = \left[\sum_{\underset{\sim}{k}_1} (\underset{\sim}{k} \times \underset{\sim}{k}_1 \cdot \hat{b})^2 |\phi_{\underset{\sim}{k}_1}(t)|^2\right]^{1/2}$$

In Fig. 9 we show the evaluation of this Doppler frequency shift compared with the frequency width measured from the Lorentzian parametrization of the spectrum. A small coefficient of 0.15 is required to reduce $\nu_D(\underset{\sim}{k})$ to the observed line width. However, the physical model for $\nu_D(\underset{\sim}{k})$ applies most appropriately to $|\underset{\sim}{k}_1| > |\underset{\sim}{k}|$ which cannot be adequately tested with the present limited number of modes.

Finally, we discuss the characteristic of the energy fluctuations W(t) as shown in Fig. 2. The energy fluctuations occur on a time scale controlled by the dissipative processes and is long compared to the oscillation period of the individual modal energies. Since each nonlinear triplet interaction conserves energy, a rapid shuffling of energy between the modes with large oscillations of $W(\underset{\sim}{k})$ occurs with no change in the total wave energy. The total energy builds up when transfer channels to the damped modes are temporarily saturated. As a result we see exponential growth at a fraction of the linear growth rate for periods of order $100\text{-}200[r_n/c_s]$ in Fig. 2. Once the total energy exceeds a certain high

level, however, the nonlinear transfer becomes sufficiently strong to force a high power transfer into damped modes. Figure 2 shows the rapid drops of $W \to W/5$ in periods of order $20\text{-}50[r_n/c_s]$. The succession of build-ups and falls in the energy is a relaxation oscillation enabling the competing modes to efficiently share the fixed input power. Increasing the input power increases the frequency of the relaxation oscillations. Increasing the number of modes in the system,[12,13] which provides more channels for the power transfer, decreases the intensity of the energy fluctuations.

V. Conclusion

We present two dimensional simulations in a low order $\underset{\sim}{k}$ space for the evolution of the fluctuations arising from the drift wave instability. We use a hydrodynamic model for the ion dynamics and a linear dissipative electron response; the model combines the principal factors of the two nonlinear models of Horton[10] and Hasegawa[11] for the description of nonlinear drift waves. The two dimensional nonlinear partial differential equation is solved in the truncated $\underset{\sim}{k}$ space introduced by Kells and Orszag in their statistical analysis of various low-order truncations of the two dimensional inviscid Navier-Stokes equation. The isotropically truncated $\underset{\sim}{k}$ space requires the evolution of 16 triplet interactions in a 20 dimensional phase space.

The simulations show a wide range of behavior, from broad band turbulence to coherent oscillation with sharply defined frequencies. The range of behavior appears to be most succinctly characterized by the value of the total growth rate $\gamma_t = \sum_{\underset{\sim}{k}} \gamma_{\underset{\sim}{k}}$. We show that the condition $\gamma_t < 0$ is necessary for the local stability of an arbitrary point in the twenty dimensional phase space. We give evidence for the condition $\gamma_t < 0$ also

being approximately a necessary and sufficient condition for the time asymptotic stability of the system. In practice for $\gamma_t < -0.1$ the amplitude of the dominant mode saturates with $|\phi_{\underset{\sim}{k}}| < 10$ in units of $(\rho/r_n)(T_e/e)$. For $\gamma_t < -0.5$ the saturated amplitudes are much less than unity.

Due to the dissipation in the system the saturated state is a state with fluctuations of the total system energy W about a mean value $\bar{W}$. As the dissipation vanishes the fluctuations of W vanish. The enstrophy that measures the mean vorticity of the flow also fluctuates even for $\gamma_{\underset{\sim}{k}} = 0$ due to the complex values of the mode coupling matrix elements. In comparison with the previous triplet studies, we find that the frequency spectra are qualitatively similar whereas the amplitudes of the twenty mode simulations are appreciably lower. We conclude that the randomly chosen triplet interactions are useful paradigms for drift wave turbulence although they are not capable of giving quantitative results for the turbulent processes.

For weakly unstable system parameters the turbulence saturates with $\tilde{\phi} < 1$. The frequency spectrum of $\phi_{\underset{\sim}{k}}(t)$ clearly shows peaks near the linear frequencies $\omega_{\underset{\sim}{k}}$ with a width that increase rapidly with $\tilde{\phi}$, approximately as $\nu \propto W \propto (\tilde{\phi})^2$.

For strongly unstable system parameters the turbulence saturates with $1 < \tilde{\phi} < 10$. The frequency spectra are broad with $\nu_{\underset{\sim}{k}} >> \omega_{\underset{\sim}{k}}$. The broad frequency spectra are peaked at a low frequency $\omega^{nl}(\underset{\sim}{k}) < 1$ which ranges from 10-50% higher than the linear frequency $\omega(\underset{\sim}{k})$. These features are shown in Figs. 7-9. The width of the spectrum ν varies approximately as $\nu \propto W^{1/2} \propto \tilde{\phi}$. The variation of the spectral width with $\tilde{\phi}$ is interpreted physically in terms of the turbulent Doppler shift model in which ν_D measures the dispersion of the linear mode frequency $\underset{\sim}{k}$, $\omega_{\underset{\sim}{k}}$ due to the turbulent flow $\underset{\sim}{v}_E(\underset{\sim}{x},t)$.

In the strong turbulence regime the mixing length estimate $e\phi/T_e \sim 1/k_x r_n$ is a commonly invoked estimate for the saturation level. In the dimensionless variables this critical mixing length turbulence level, $\tilde{\phi}_M$, interpreted in terms of the dominant k_x mode in the saturated spectrum ($k_x = 2k_0$ gives $\tilde{\phi}_M = 1/k_x = 1/2k_0 \sim 1.5$ which compares with the observed levels $\tilde{\phi} = 2$ to 20 for $\gamma_t = -.44$ to -0.1. Alternatively, the fluctuation level given by Horton[10] also varies inversely with k_x as in the mixing length theory and is proportional to $\delta_0^{1/2}$ due to the driving term of the turbulence. The simulations show that there is a dependence of $\tilde{\phi}$ on k_x and δ_0 which is more nearly consistent with the dissipative estimate rather than the simple mixing length estimate.

In a future investigation we will report on work in progress using the random phase approximation to compute the averaged values of the spectral energies. Due to the relatively small number of $\underset{\sim}{k}$ modes in the present model, the results for the distribution of energy in $\underset{\sim}{k}$ space are principally qualitative. The model shows that the broad frequency spectra are not related to the number of $\underset{\sim}{k}$ modes in the system. As suggested by the prototype of a single triplet interaction chosen randomly from a continuous $\underset{\sim}{k}$ space, the broad frequency spectrum is directly related to the presence of dissipation in the system. The anisotropy of the wavenumber spectrum is shown to result from the driving mechanism $\gamma_{\underset{\sim}{k}}$ which is peaked along $k_x = 0$ competing with the isotropizing effect of the convective mode coupling process. In the dissipative system the time averaged wavenumber spectrum $W(\underset{\sim}{k})$ is a unique structure, stable to large perturbations which arises from a large basin of attraction in the 20 dimensional phase space.

Acknowledgments

The authors wish to acknowledge the efficient work of Mr. Lee Leonard in performing the numerical simulations. The authors are grateful to Drs. M. N. Rosenbluth and D. Biskamp for useful discussions.

This work was supported by the Department of Energy Contract Number DE FG05-80ET-53088.

REFERENCES

1. E.N. Lorenz, J. Atmos. Sci. 20, 130(1963).

2. D. Ruelle and F. Takens, Comm. Math. Phys. 20, 167(1971).

3. J.B. McLaughlin and P.C. Martin, Phys. Rev. A12, 186(1975).

4. L.C. Kells and S.A. Orszag, Phys. Fluids 21, 162(1978).

5. S. Ya. Vyshkind and M.I. Rabinovich, Zh. Eksp. Theor. Fiz. 71, 557(1976) [Sov. Phys. -JETP 44, 292(1976)].

6. J.M. Wersinger, J.M. Finn, and E. Ott, Phys. Fluids 23, 1142(1980).

7. P.K.C. Wang and K. Masui, Phys. Lett. 81A, 97(1981).

8. P. Terry and W. Horton, Phys. Fluids 25, 491(1982).

9. M.N. Bussac, "The Nonlinear Three Wave System, Strange Attractors and Asymptotic Solutions" preprint (1982) and Physica D, 236(1982).

10. W. Horton, Phys. Rev. Lett. 37, 1269(1976).

11. A. Hasegawa and K. Mima, Phys. Rev. Lett. 39, 205(1977).

12. R. E. Waltz, in Proceedings of the U. S. Japan Workshop on Drift Wave Turbulence, Institute for Fusion Studies, IFS#53, 195 (1982).

13. D. Brock and W. Horton, Plasma Physics 24, 271(1982). 1982).

FIGURE CAPTIONS

1. The isotropically truncated wavenumber space of twenty modes.

2. Time evolution of the energy W(t) and enstrophy U(t) from an initial state of randomly phased amplitudes with $|\phi_{\underset{\sim}{k}}| = 0.1$.

3. Mean saturation amplitude of the fastest growing linear mode ϕ_7 and the dominant mode ϕ_9 as a function of γ_t, the sum of the growth rates.

4. Time evolution of the fastest growing linear mode ϕ_7 and the dominant mode ϕ_9 for a weakly unstable case ($\gamma_t = -.35$).

5. Stationary wavenumber spectrum for weakly unstable case ($\gamma_t = -.35$).

6. Isotropic stationary spectrum obtained by switching off the linear growth rates $\gamma_{\underset{\sim}{k}}$ after $\Delta t = 2000$.

7. Frequency spectra $|\phi_7(\omega)|$ and $|\phi_9(\omega)|$ of the fastest growing linear mode and the dominant mode for a weakly unstable case ($\gamma_t = -.30$).

8. Frequency spectra $|\phi_7(\omega)|$ for a strongly unstable case ($\gamma_t = - .131$).

9. Linewidth of the frequency spectrum as a function of the saturation amplitude of mode ϕ_9.

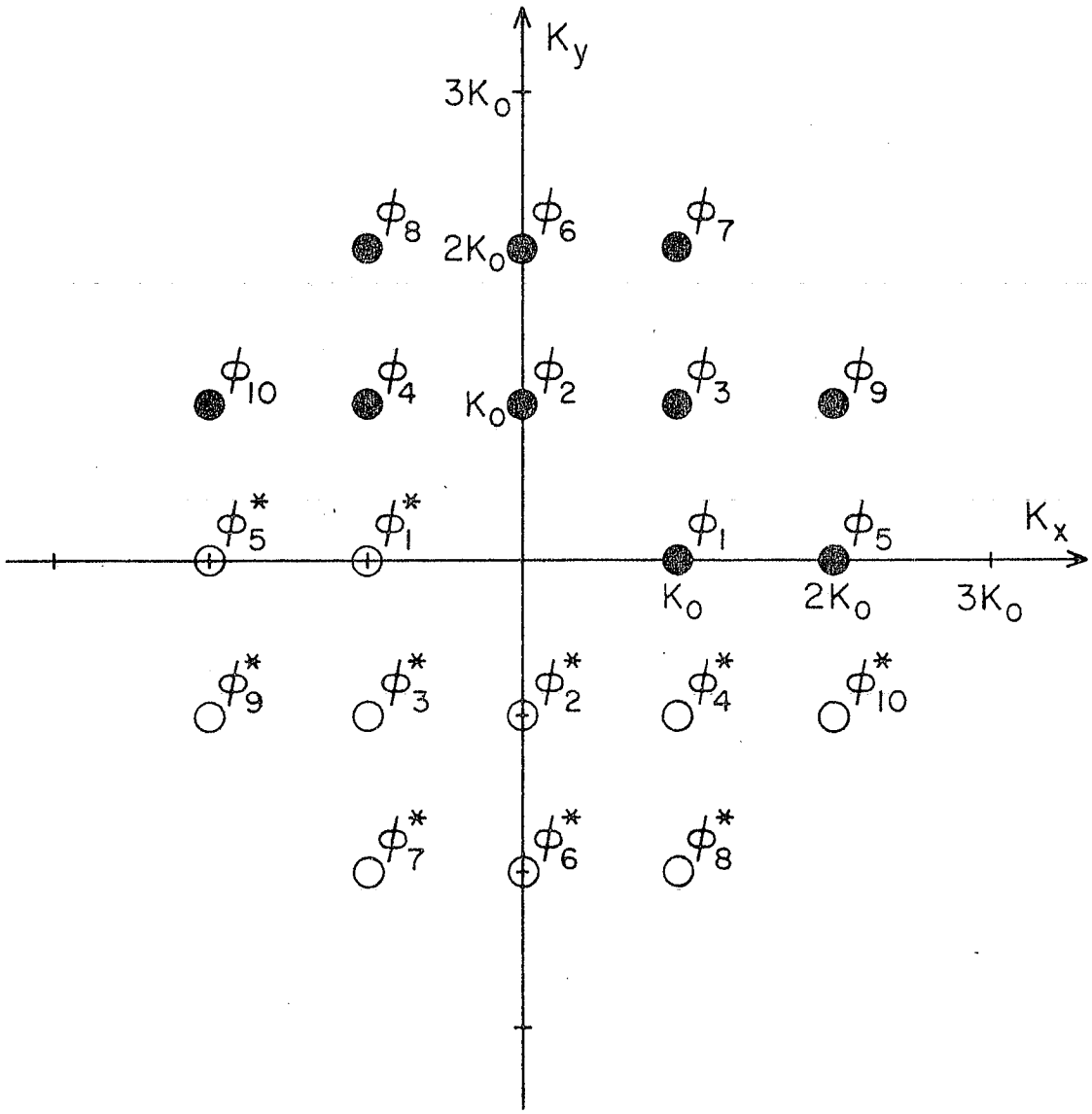
K_y
$3K_0$
$2K_0$
K_0
K_x
$2K_0$
$3K_0$
ϕ_8
ϕ_6
ϕ_7
ϕ_{10}
ϕ_4
ϕ_2
ϕ_3
ϕ_9
ϕ_5^*
ϕ_1^*
ϕ_1
ϕ_5
ϕ_9^*
ϕ_3^*
ϕ_2^*
ϕ_4^*
ϕ_{10}^*
ϕ_7^*
ϕ_6^*
ϕ_8^*

FIG. 1

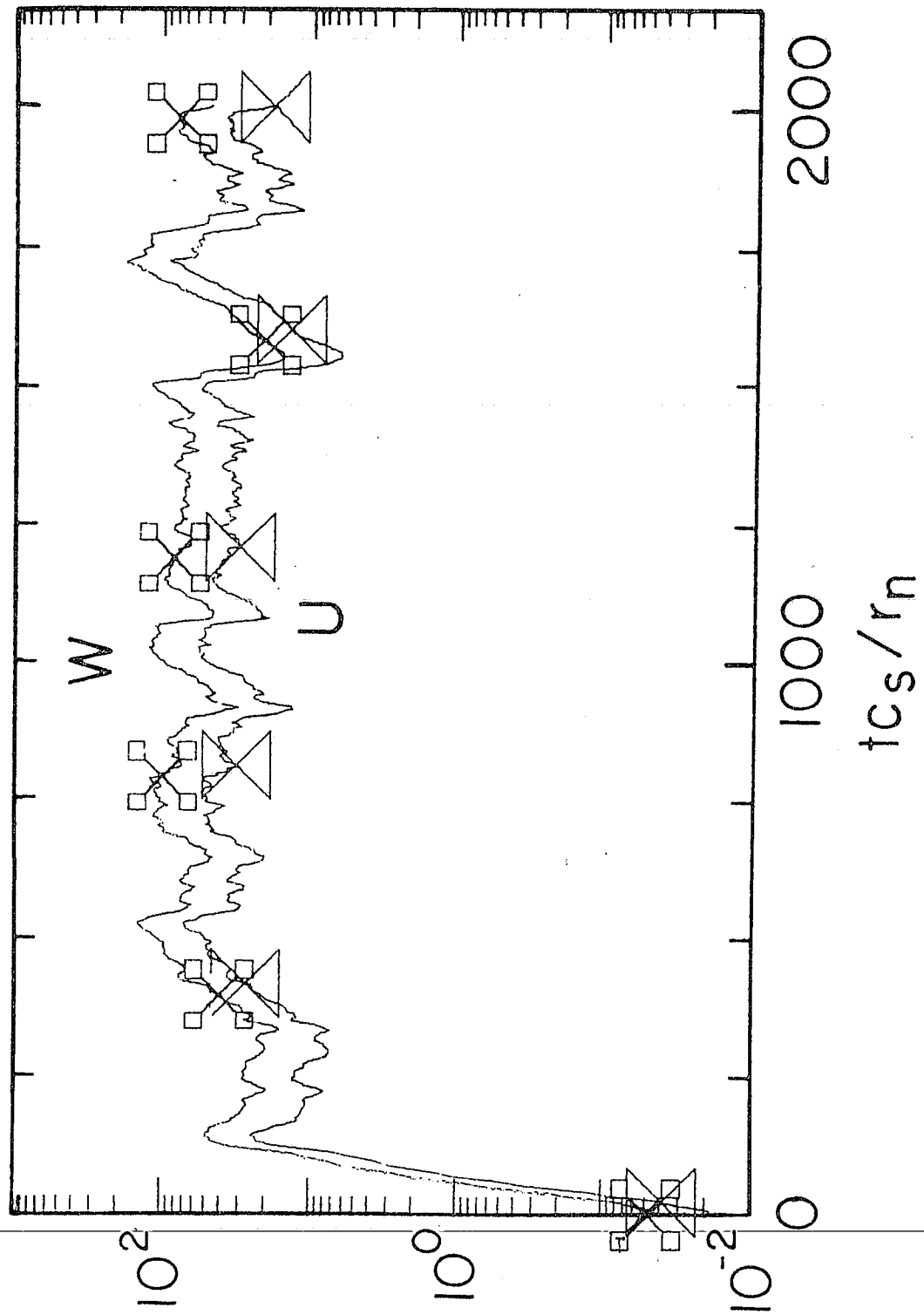

FIG. 2

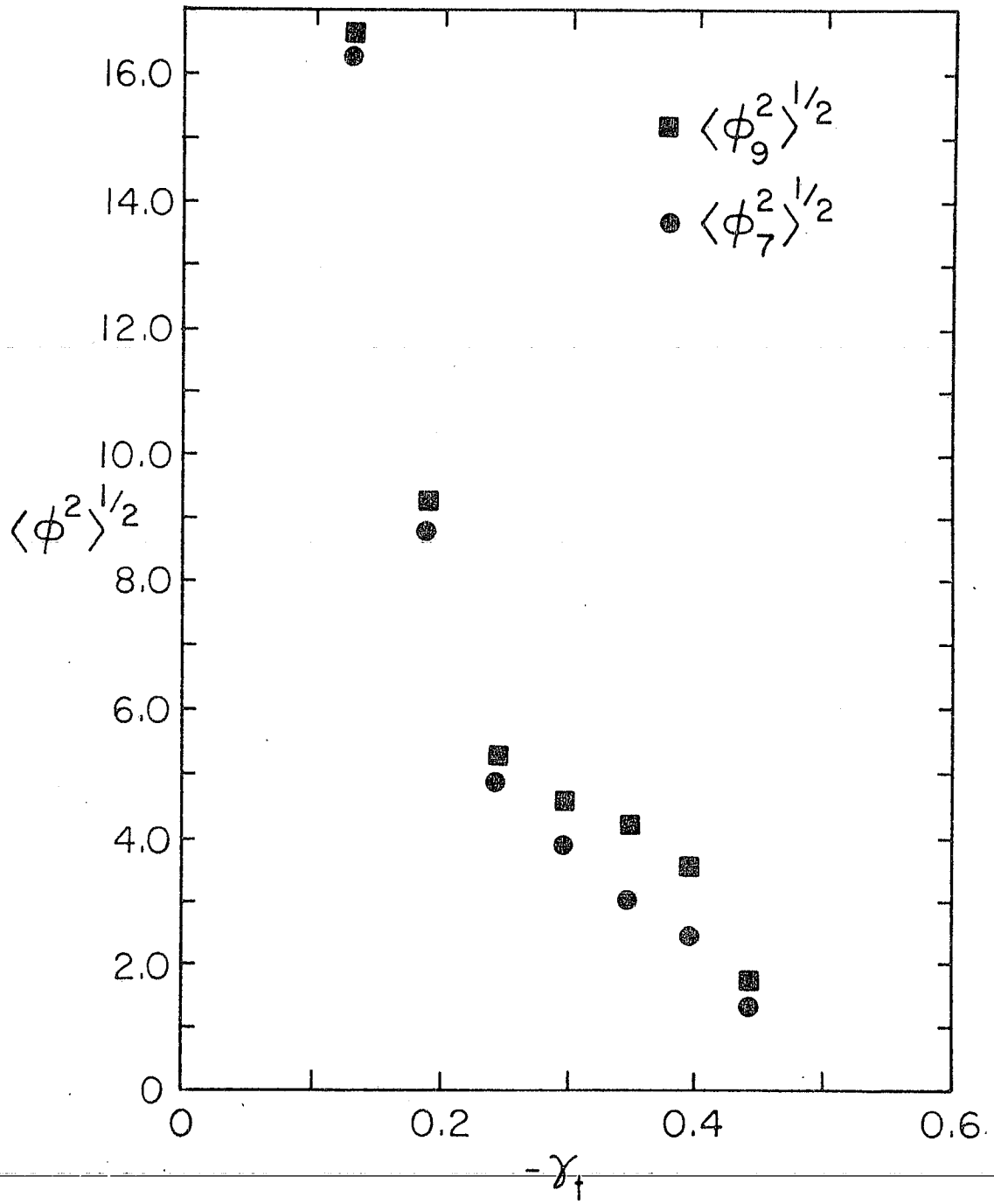
16.0
14.0
12.0
10.0
8.0
6.0
4.0
2.0
0
0
0.2
0.4
0.6
$\langle\phi^2\rangle^{1/2}$
$-\gamma_t$
$\langle\phi_9^2\rangle^{1/2}$
$\langle\phi_7^2\rangle^{1/2}$

FIG. 3

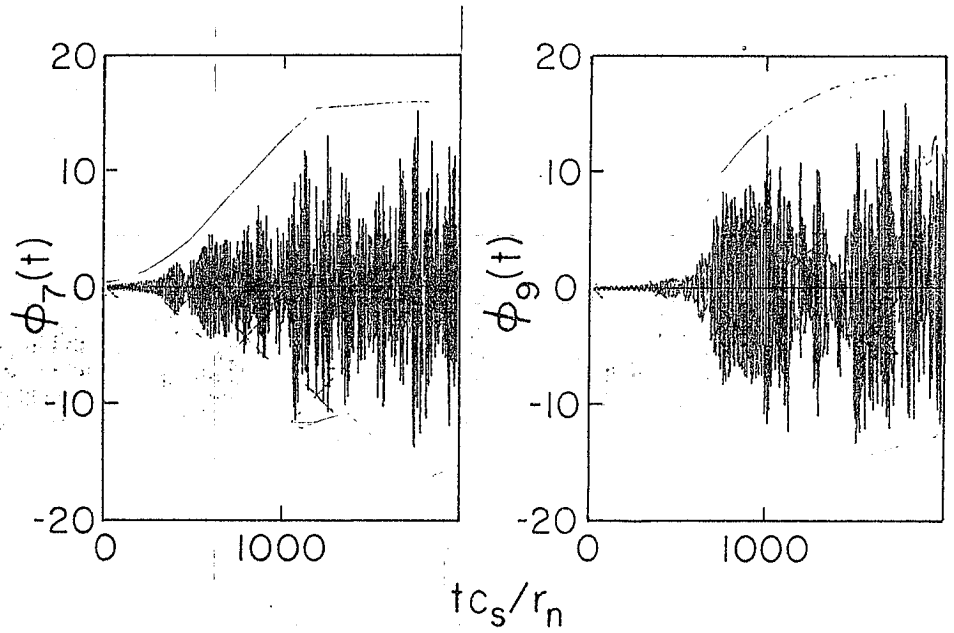

FIG. 4

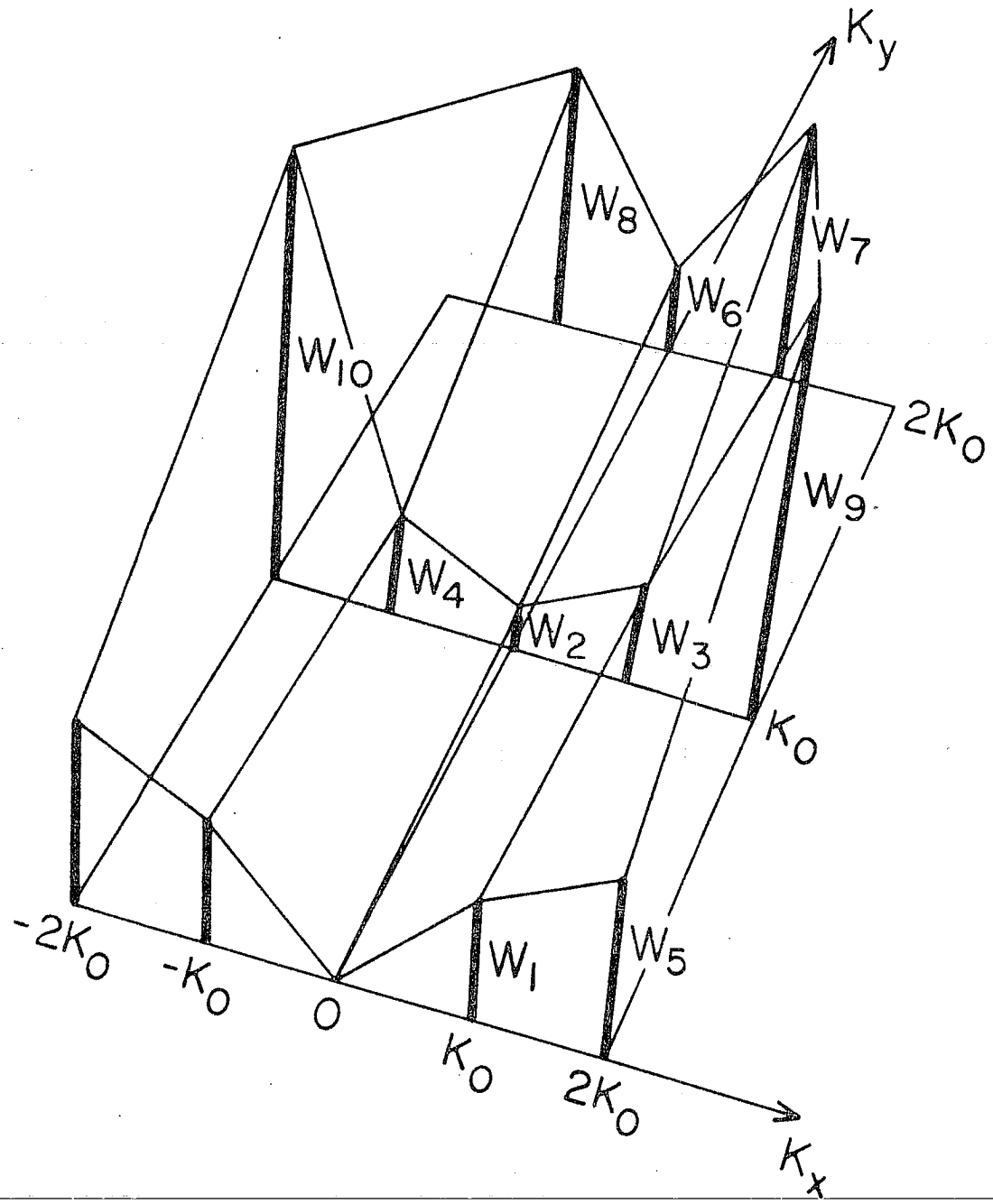

FIG. 5

$\overline{W} = 40 \quad \Delta t = 2000$

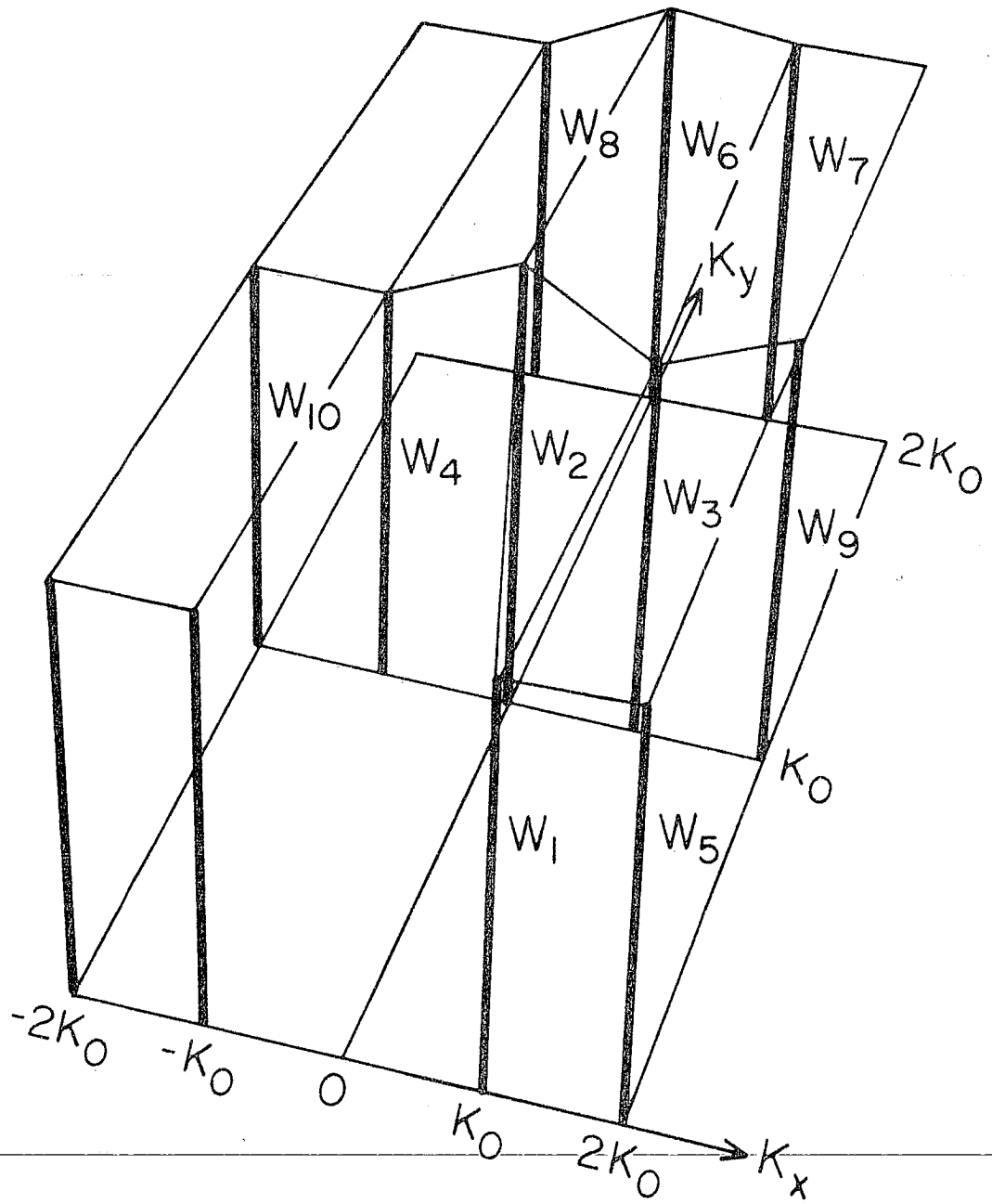

FIG. 6

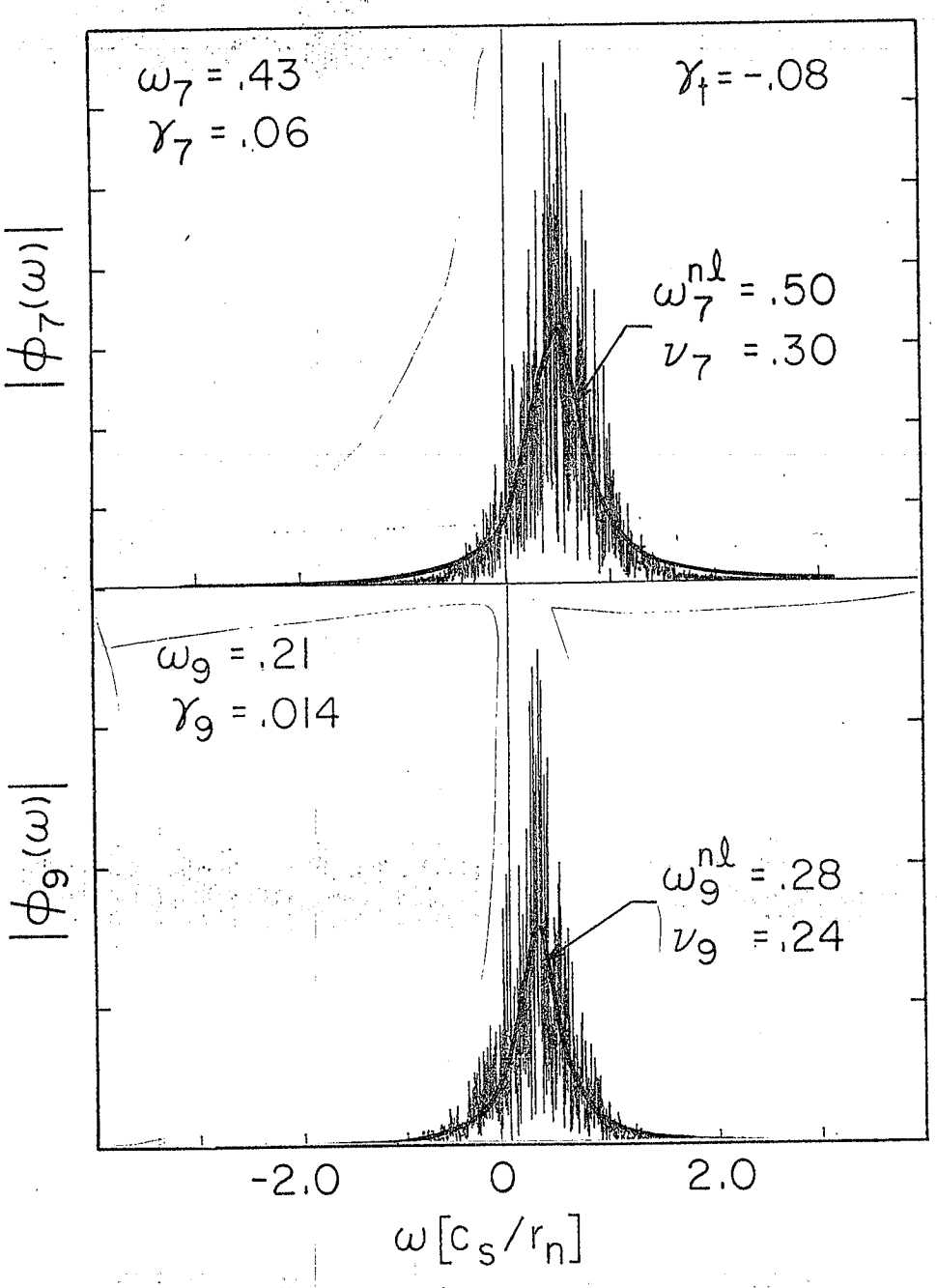
$\omega_7 = .43$
$\gamma_7 = .06$
$\gamma_7 = -.08$
$\omega_7^{nl} = .50$
$\nu_7 = .30$
$|\phi_7(\omega)|$
$\omega_9 = .21$
$\gamma_9 = .014$
$\omega_9^{nl} = .28$
$\nu_9 = .24$
$|\phi_9(\omega)|$
-2.0
0
2.0
$\omega [c_s/r_n]$

FIG. 7

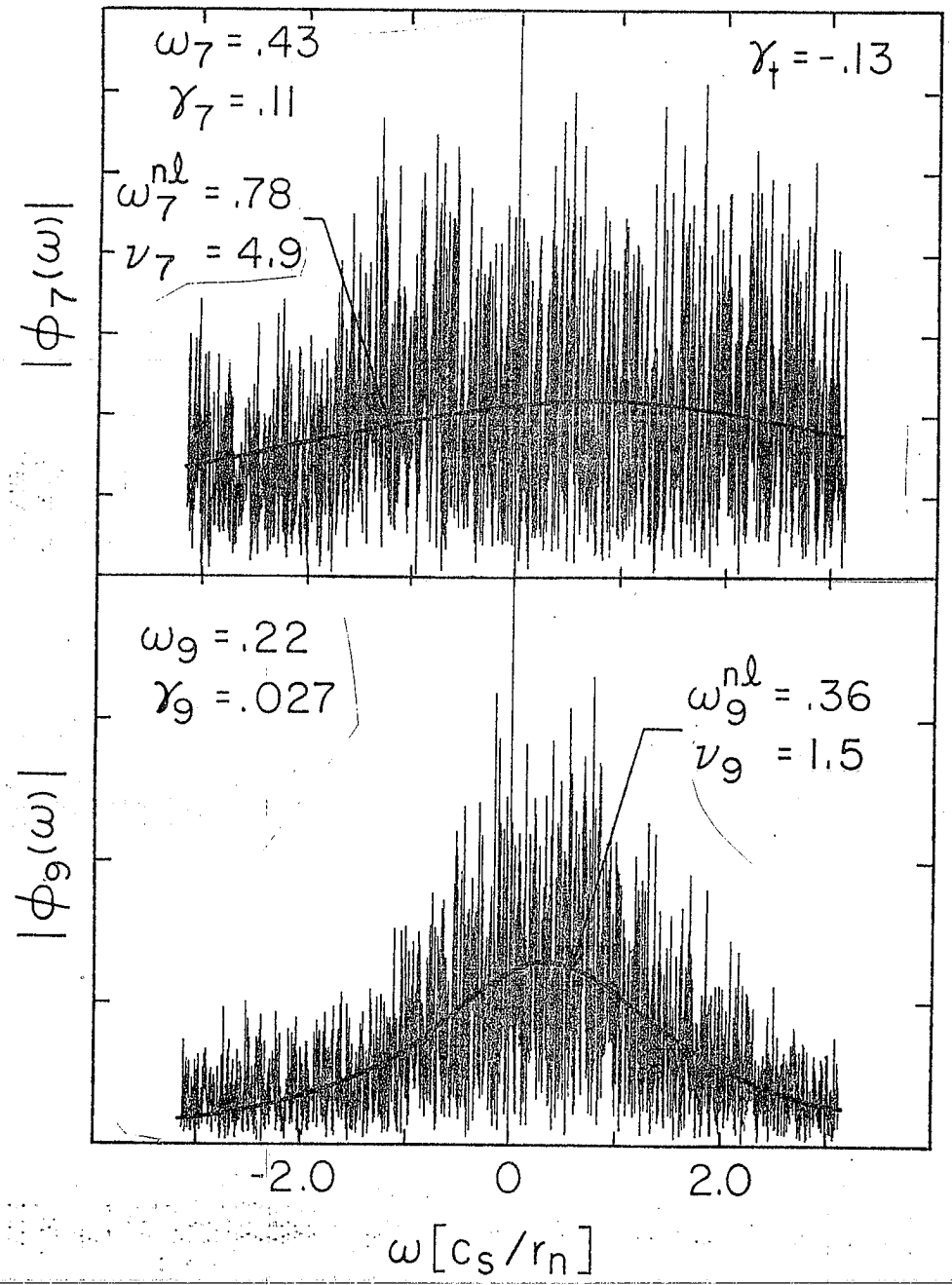
$\omega_7 = .43$
$\gamma_7 = .11$
$\omega_7^{nl} = .78$
$\nu_7 = 4.9$
$\gamma_t = -.13$
$|\phi_7(\omega)|$
$\omega_9 = .22$
$\gamma_9 = .027$
$\omega_9^{nl} = .36$
$\nu_9 = 1.5$
$|\phi_9(\omega)|$
-2.0
0
2.0
$\omega[c_s/r_n]$

FIG. 8

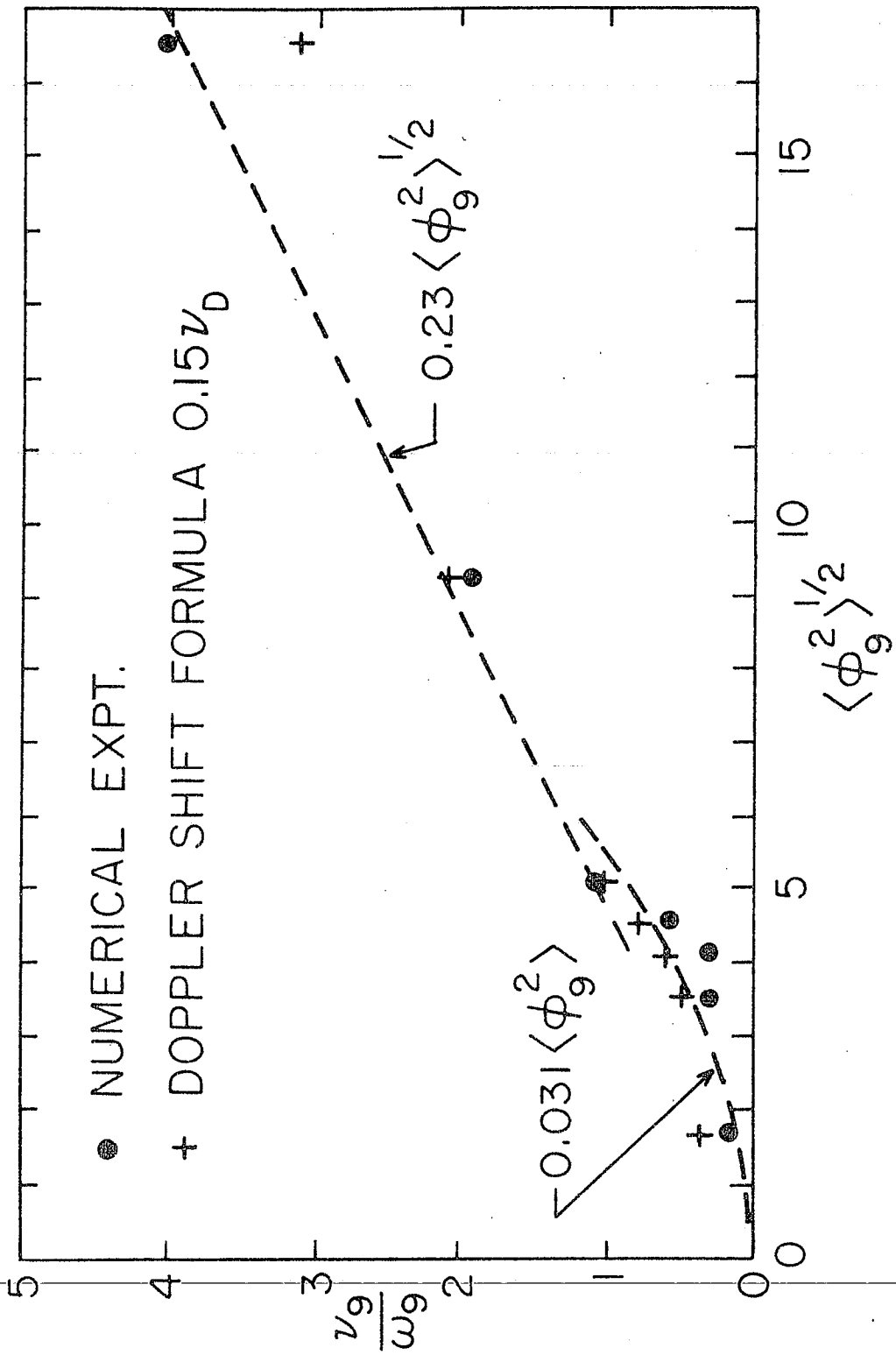
• NUMERICAL EXPT.
+ DOPPLER SHIFT FORMULA 0.15ν_D
0.23$\langle\phi_9^2\rangle^{1/2}$
0.031$\langle\phi_9^2\rangle$
$\frac{\nu_9}{\omega_9}$
$\langle\phi_9^2\rangle^{1/2}$
0
1
2
3
4
5
0
5
10
15

FIG. 9